31st Annual International Conference of the IEEE EMBS
Minneapolis, Minnesota, USA, September 2-6, 2009

3D Polarization-Sensitive Optical Coherence Tomography of Canine Meniscus Based on a 2D High-Fill-Factor Microelectromechanical Mirror

Shuguang Guo, Jingjing Sun, *Student Member, IEEE*, Antonio Pozzi, Hang-yin Ling, Lei Wu, *Student Member, IEEE,* Lin Liu, and Huikai Xie, *Senior Member, IEEE*

***Abstract*—A miniature optical imaging probe based on a high-fill-factor MEMS mirror has been developed for nondestructive diagnosis of articular joint diseases and injuries. The MEMS mirror scans ±30° at less than 6 V in both x- and y-axis. The outer diameter of the probe is 5.8 mm. Three-dimensional polarization-sensitive optical coherence tomography of canine meniscus has been successfully demonstrated.**

I. Introduction

Osteoarthritis (OA) is a musculoskeletal disease that is causing pain and disability to ~70 million people in US alone[1]. The most common articular lesions leading to the progressive development of cartilage defects and OA are meniscal tears. Magnetic resonance imaging (MRI) is usually performed for diagnosis but conventional MRI offers limited resolution and contrast. Optical coherence tomography (OCT), on the other hand, can provide high-resolution cross-sectional images of highly-scattering biological tissues [2]. OCT can obtain ~10 μm resolutions and 1~3 mm imaging depths. By extracting polarization information, polarization-sensitive OCT (PS-OCT) can significantly increase the image contrast to tissue samples with strong birefringence. Study has shown that menisci have strong birefringence due to the orientation and organization of their collagen fibril networks [3][4]. PS-OCT has been applied to bovine articular cartilage and meniscus [5]-[7]. However, it is challenging to apply PS-OCT for in vivo arthroscopic imaging due to the requirements of small probe size and fast image speed. The most critical part in this type of application is the transverse light beam scanning. Several transverse scanning methods have been reported [8]-[12], but they have limitations such as low coupling stability, slow speed, large size, or non-uniformity.

MEMS devices typically have small size and high speed, making them ideal for miniaturizing OCT probes. A few research groups have demonstrated promising results by combining MEMS micromirrors with OCT [13]-[21]. The transverse scanning can be based on electrothermal [13]-[15], electrostatic [16]-[19] or electromagnetic [20][21] actuation. The common problem for most existing MEMS mirrors is the small fill factors which are only about 5%. Using MEMS mirrors with small fill factors will result in large imaging probe sizes. Therefore, one of the challenges for OCT probe miniaturization is to develop MEMS mirrors with high fill factors.

In this paper, we report the 3D PS-OCT imaging results of a handheld OCT probe based on a MEMS mirror with a fill factor as high as 25%.

II. MEMS Mirror

In order to achieve high fill factor without using complicated multi-wafer bonding or mirror transfer process, electrothermal bimorph actuation is chosen. As shown in Fig. 1(a), the mirror plate is supported by four identical bimorph (Al/SiO_2) actuators on the four sides. Each actuator has three bimorph segments that are folded to reduce the actuator area and thus increase the fill factor [15]. A Pt heater is embedded in each actuator for electrothermal actuation. The initial elevation of the mirror plate is caused by the residual stress inside the bimorph beams and the mirror plate moves downward upon electrothermal actuation. This design can achieve a tip-tilt-piston motion with the tip-tilt scanning generated by differentially driving the two opposite actuators and the piston motion by simultaneously driving the four actuators. The compactly-folded actuators enable a high fill factor of 25% with a large mirror aperture of 1×1 mm^2 on a device footprint of only 2×2 mm^2. Fig. 1(a) shows the SEM of a fabricated MEMS mirror. The fabricated mirror demonstrated optical scan angles of ±30º at the driving voltage of only 5.5 V, as shown in Fig. 1(b).

Manuscript received April 23, 2009. This work was supported in part by National Science Foundation under award#0725598, the Research Development Fund of the College of Veterinary Medicine in University of Florida, and the University of Florida Research Foundation.

S. Guo, J. Sun, L. Wu, L. Liu and H. Xie are with the Department of Electrical and Computer Engineering, University of Florida, Gainesville, FL 32611 USA (corresponding author J. Sun phone: 352-871-6812; e-mail: sunjingjingmia@ufl.edu).

A. Pozzi is with Department of Small Animal Clinical Sciences, University of Florida, Gainesville, FL 32610, USA (e-mail: PozziA@vetmed.ufl.edu).

H. Ling is with Department of Orthopaedics and Rehabilitation, University of Florida, Gainesville, FL 32607, USA (e-mail: lingch@ortho.ufl.edu).

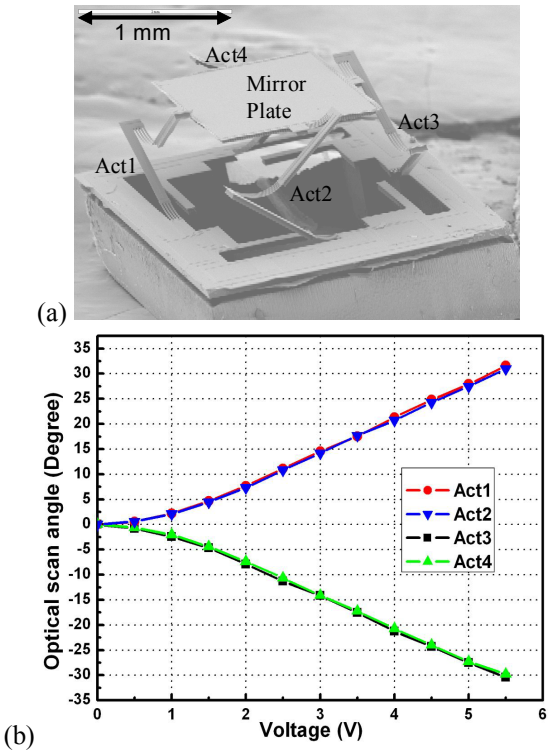

Fig. 1. (a) An SEM picture of a fabricated micromirror. (b) Optical scan angles vs. voltage applied on each actuator.

III. MEMS-BASED OCT PROBE

The packaging scheme of the OCT probe is illustrated in Fig. 2(a), where all the micro-optical components are installed into a high-precision-machined cylindrical vessel. The jacket of the distal tip of the optical fiber is stripped off and the fiber is cut with an angle of 8 degree to avoid the Fresnel backreflection. A GRIN lens with a diameter of 700 μm is employed to focus the sample optical beam. The working distance of the probe can be adjusted by controlling the distance between the fiber and the GRIN lens. A 2D MEMS micromirror (Fig. 1(a)) is assembled into a square pocket in the vessel. The loaded vessel is slipped into a flexible biocompatible transparent fluorinated ethylene propylene (FEP) tube. The diameter of the cylindrical vessel is 5 mm. The total outer diameter of the probe is 5.8 mm. Figs. 2(b), 2(c) and 2(d) respectively show the close view of the packaged probe without the FEP tube, the packaged probe with a US dime, and the probe in OCT imaging of a canine meniscus.

IV. PS-OCT SYSTEM

The balanced-detection PS-OCT system is shown in Fig. 3. The light source has a central wavelength of 1310 nm and FWHM of 75 nm, corresponding to 10 μm axial resolution in free space. The output light is polarized to 45° with respect to the optical axis of the crystal inside the polarization modulator that is driven by a square-wave voltage to generate periodic phase shifts of zero and π/2. The corresponding two Stokes vectors of the output light are orthogonal in the Poincaré sphere representation so that the birefringence measurements are independent of the orientation of the optical axis in the sample. In the detection arm, the returning optical beam is split into two polarization channels. The scanning rate of the optical delay line is 1 kHz. The rapid scanning mirror in the delay line is laterally shifted to generate a carrier frequency of 500 kHz. The interference fringe signals from the two polarization channels are detected by two balanced photodetectors (BPD) and the BPD output signals are streamed into a PC via a high speed data acquisition board. The phase resolved method [22][23] is employed to calculate structural and polarization sensitive images.

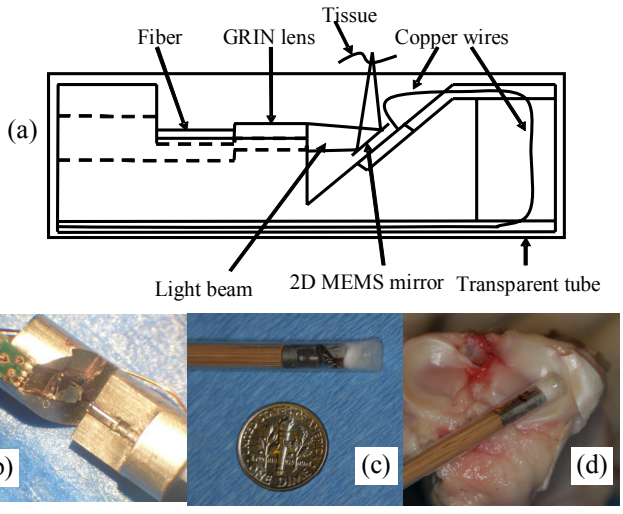

Fig. 2. OCT probe packaging. (a) Cross-sectional view (along the tube). (b) A close view of the probe without the FEP tube. (c) A packaged probe with a US dime. (d) OCT imaging of a canine meniscus.

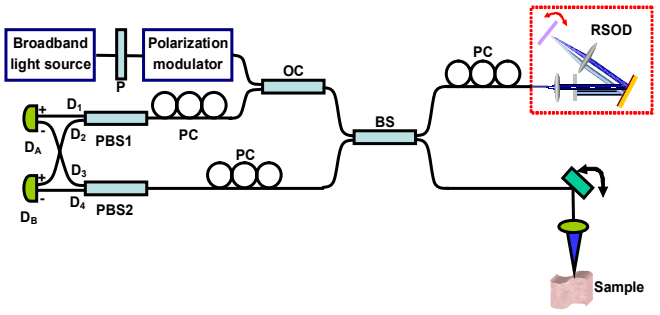

Fig. 3. Schematic diagram of the polarization sensitive optical coherence tomography. P: polarizer; OC: optical circulator; PC: polarization controller; RSOD: rapid scanning optical delay line; BS: 2 × 2 beam splitter; PBS: polarization beam splitter; D_A and D_B: balanced photodetectors.

V. RESULTS

Ex vivo 2D and 3D PS-OCT imaging of a canine meniscus have been performed to show the capability of the system. A canine knee joint was cut open (Fig. 2(d)) to expose the menisci. The packaged OCT probe was positioned at different locations of the menisci. A lateral scanning area of 2.3 × 2.3 mm^2 was obtained by driving two opposite pairs of the actuators with two sets of voltages, *i.e.,* 0~4 V for the circumferential direction scanning and 0.5~3.5 V for the longitudinal direction scanning.

Fig. 4 shows 2D and 3D PS-OCT images of the canine meniscus. The 2D Stokes parameter images, corresponding to *I*, *U*, *V* and *Q*, respectively, are shown in Fig. 4(a), where each row represents one of the two polarization states. Fig. 4(b) shows the 3D OCT reconstructed from the intensity parameter *I*. The measured axial resolution (FWHM) of the structural image is 11.2μm in air. For PS-OCT images, accumulated double-pass phase retardation images are often employed to represent the tissue birefringence, but this requires a strong surface signal as reference. In our case, the surface signal is relatively weak. So, only one of the Stokes parameter images, *Q*, is used to reconstruct the 3D PS-OCT image instead of using the phase retardation image, as shown in Fig. 4(c).

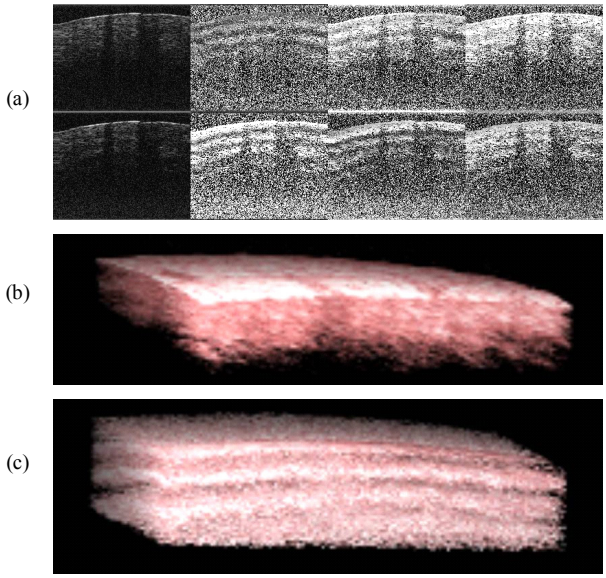

Fig. 4. (a) 2D Stokes parameters images (2.3×1.6 mm^2). (b) 3D OCT (2.3×2.3×1.6mm^3). (c) 3D PSOCT (2.3×2.3×0.8mm^3) of a canine meniscus.

The two shadowed areas in Fig. 4(a) are artifacts due to two blots on the FEP tube. It is noticed that a flat surface of the sample will be slightly curved in the 2D OCT image. This is because the center of the MEMS mirror is not located at the center of the light beam. Also the path length difference due to the circumferential and longitudinal scanning is not compensated. Birefringence measurement will be affected by the same reasons. In addition, the tissue birefringence property measured with the MEMS-based probe will be slightly different from the case where a lateral scanning stage is used since the birefringence is orientation- dependant. Furthermore, by observing the polarization states of the light backscattered from the inner and outer surfaces of the FEP tube, we have noticed that the FEP tube also exhibits certain birefringence, which varies due to different path-lengths between the two tube surfaces at different locations. Thus the polarization states backscattered from the sample also varied slightly along the lateral scanning direction.

VI. CONCLUSION

A 5.8mm-diameter miniature handheld OCT probe based on a high-fill-factor MEMS mirror has been designed, manufactured and packaged. This high-fill-factor MEMS mirror design can be used to further reduce the diameter of OCT probes. Three-dimensional PS-OCT of a canine meniscus has been successfully obtained using the MEMS OCT probe. This PS-OCT probe design is promising for nondestructive arthroscopic diagnosis and intervention of various articular joint diseases and injuries. The artifacts of the OCT images will be corrected via signal processing in the future. The next generation probe with smaller diameter is being developed in our group.

REFERENCES

[1] www.arthritis.org

[2] D. Huang, E. A. Swanson, C. P. Lin, J. S. Schuman, W. G. Stinson, W. Chang, M. R. Hee, T. Flotte, K. Gregory, C. A. Puliafito, J. G. Fujimoto, "Optical coherence tomography," Science, vol.254 (1991), no.5035, pp.1178-1181.

[3] T. Xie, S. Guo, J. Zhang, Z. Chen, G.M. Peavy, "Use of PS-OCT to determine the directional polarization sensitivity of articular cartilage and meniscus", J. Biomedical Optics 064001(2006).

[4] W. Drexler, D. Stamper, C. Jesser, X. Li, C. Pitris, et al., "Correlation of collagen organization with polarization sensitive imaging of in vitro cartilage: implications for osteoarthritis", J Rheumatol, vol. 28, pp. 1311-1318, 2001.

[5] T. Xie, S. Guo, J. Zhang, et al, "Use of polarization-sensitive optical coherence tomography to determine the directional polarization sensitivity of articular cartilage and meniscus," J Biomed Opt 11(6), 064001-1-8 (2006).

[6] J. M. Herrman, C. Pitris, B. E. Bouma, et al., "High resolution imaing of normal and osteoarthritic cartilage with optical coherence tomography", J Rheumatol, vol. 26 (1999) 627-35.

[7] C. R. Chu, D. Lin, J. L. Geisler, C. T. Chu, F. H. Fu and Y. Pan, "Arthroscopic microscopy of articular cartilage using OCT", The American Journal of Sports Medicine, vol. 32, pp. 699-709, 2004.

[8] G. J. Tearney, M. E. Brezinski, B. E. Bouma, S. A. Boppart, C. Pitris, J. F. Southern, and J. G. Fujimoto, "*In Vivo* Endoscopic Optical Biopsy with Optical Coherence Tomography," Science 276, 2037-2039 (1997).

[9] A.M. Sergeev, V. M Gelikonov, G.V. Gelikonov, F. I. Feldchtein, and R. V. Kuranov, "*In vivo* endoscopic OCT imaging of precancer and cancer states of human mucosa," Opt. Express 1 (1997) 432-440.

[10] Y. Wang, M. Bachman, G. -P. Li, S. Guo, B. J. F. Wong, and Z. Chen, "Low-voltage polymer-based scanning cantilever for *in vivo* optical coherence tomography," Opt. Lett. 30, 53-55 (2005).

[11] X. Liu, M. J. Cobb, Y. Chen, M. B. Kimmey, and X. Li, "Rapid-scanning forward-imaging miniature endoscope for real-time optical coherence tomography," Opt. Lett. 29, 1763-1765 (2004).

[12] J. Wu, M. Conry, C. Gu, F. Wang, Z. Yaqoob, and C. Yang, "Paired-angle-rotation scanning optical coherence tomography forward-imaging probe," Opt. Lett. 31, 1265-1267 (2006).

[13] Y. Pan, H. Xie and G.K. Fedder, "Endoscopic optical coherence tomography based on a microelectromechanical mirror," Optics Letters, 26 (2001) 1966-1968.

[14] H. Xie, Y. Pan and G.K. Fedder, "Endoscopic opical coherence tomographic imaging with a CMOS MEMS micromirror," Sensors & Actuators: A, 103 (2003), 237 – 241.

[15] L. Wu and H. Xie, "A large vertical displacement electrothermal bimorph actuator with very small lateral shift", Sensors and Actuators A 145-146, 371-379 (2008).

[16] B. Qi, A.P. Himmer, L.M. Gordon, X.D. Yang, L.D. Dickensheets, I.A. Vitkin, "Dynamic focus control in high-speed optical coherence tomography based on a microelectromechanical mirror," Optics Communications, vol. 232 (2004), pp. 123–128.

[17] J. M. Zara, S. Yazdanfar, K. D. Rao, J. A. Izatt, and S. W. Smith, "Electrostatic Micromachine Scanning Mirror for Optical Coherence Tomography," Optics Letters, vol. 22, pp. 628-630, 2003.

[18] L. S. Fan, W. Piyawattanametha, M. C. Wu, A. D. Aguirre, P. R. Herz, Y. Chen, and J. G. Fujimoto, "High-resolution 3D OCT Imaging with a MEMS Scanning Endoscope," Proceedings of the SPIE, vol. 5719, pp. 140-143, 2005.

[19] D. T. McCormick, W. Jung, Z. Chen, and N. C. Tien, "3-D MEMS Based Minimally Invasive Optical Coherence Tomography," Technical Digest of the 13th International Conference on Solid-State Sensors, Actuators and Microsystems (Transducers 2005), Seoul, Korea, 2005.

[20] K.H. Kim, B. H. Park, G. N. Maguluri, T. W. Lee, F. J. Rogomentich, M. G. Bancu, B. E. Bouma, J. F. de Boer, and J. J. Bernstein, "Two-axis magnetically-driven MEMS scanning catheter for endoscopic high-speed optical coherence tomography," Optics Express, 15 (2007), pp. 18130-18140.

[21] J.J. Bernstein, T.W. Lee, F.J. Rogomentich, M.G. Bancu, K.H. Kim, G. Maguluri, B.E. Bouma, and J.F. DeBoer, "Magnetic two-axis micromirror for 3D OCT endoscopy," Technical Digest of Solid-State Sensors, Actuators, and Microsystems Workshop (Hilton Head 2006), Hilton Head Island, SC, June 4-8, 2006, pp. 7-10.

[22] Y. Zhao, Z. Chen, C. Saxer, S. Xiang, J. de Boer, and J. Nelson, "Phase Resolved Optical Coherence Tomography and Optical Doppler Tomography for Imaging blood flow in human skin with fast scanning speed and high velocity sensitivity," Opt. Lett. 25, 114 (2000).

[23] H. Ren, Z. Ding, Y. Zhao, J. Miao, J. Nelson, and Z. Chen, "Phase-resolved functional optical coherence tomography: simultaneous imaging of in situ tissue structure, blood flow velocity, standard deviation, birefringence, and Stokes vectors in human tissue," Opt. Lett. 27, 1702-04 (2002).